Scientific Research Publishing

Geomaterials, 2022, 12, 70-92
https://www.scirp.org/journal/gm
ISSN Online: 2161-7546
ISSN Print: 2161-7538

Development and Testing of a Method to Estimate the Mineral Composition of Ore from Chemical Assays with a View toward Geometallurgy: Application to an Iron Ore Concentrator

Laurence Boisvert[1], Claude Bazin[1], Josiane Caron[2], François Lavoie[2]

[1]Department of Mining, Metallurgical and Material Engineering, Laval University, Quebec City, Canada
[2]Quebec Iron Ore, Fermont, Canada
Email: laurence.boisvert.1@ulaval.ca, claude.bazin@gmn.ulaval.ca, JCaron@MineraiFerQuebec.com, FLavoie@MineraiFerQuebec.com

How to cite this paper: Boisvert, L., Bazin, C., Caron, J. and Lavoie, F. (2022) Development and Testing of a Method to Estimate the Mineral Composition of Ore from Chemical Assays with a View toward Geometallurgy: Application to an Iron Ore Concentrator. *Geomaterials*, **12**, 70-92.
https://doi.org/10.4236/gm.2022.124006

Received: August 2, 2022
Accepted: September 26, 2022
Published: September 29, 2022

Abstract

For complex orebodies in which the valuable metal is carried by several minerals that respond differently to the concentration process, an ore block model should not be characterized solely with elemental assays, as this information is not sufficient to anticipate the mill performances. Data from an iron ore concentrator is used to demonstrate the idea. A method is then proposed to estimate the mineral contents of ore samples from elemental assays. The method can readily be extended to combine the estimation of the mineral contents in the feed of the mill with an estimation of the recovery of these minerals into the products of the concentrator. These mineral recoveries can subsequently be incorporated into a block model to predict the concentrator response to the processing of an ore block.

Keywords

Block Model, Estimation, Geometallurgy, Iron Ore Concentrator, Mill Performance, Mineral Content, Modal

1. Introduction

The ore blocks of a mine block model are usually characterized by metal contents such as gold (g/t), copper (%), or iron (%) grades. In some applications, information concerning ore hardness or grindability and mineral processing

responses is incorporated into the block model in order to use the block model for geometallurgical predictions [1] [2] [3]. However, few papers report that the ore of a block model should be characterized in terms of mineral contents and indices describing the way these minerals are separated by the concentrator. This is somehow surprising as mineral processing plants separate the minerals and not the elements. This paper describes with an example taken from an iron ore mine the advantages of describing an ore block by its mineral composition rather than its elemental composition and discusses approaches to estimate a mineral composition from the usual elemental assays of ore samples and to estimate the recovery of the minerals in a concentrator.

The paper is divided into 4 sections. The first section discusses the research purposes, objectives and steps followed in the paper. The second section briefly describes the operation of the Quebec Iron Ore (QIO) iron ore mine in Canada, used to illustrate the discussion presented in the paper. The third section shows the advantage of using mineral assays for an ore block model rather than elemental assays for the considered iron ore mine. The fourth section reviews methods to estimate the mineral contents of an ore sample and the fourth section proposes an approach to estimate from daily production samples collected in the concentrator, the way minerals are separated in the concentration circuit. This last information complements the mineral characteristics of an ore block model for a geometallurgy application.

2. Steps in the Development of a Geometallurgical Tool Based on the Ore Mineral Composition

Figure 1 shows the two main steps followed here. The first step is the development and testing of a tool to estimate the mineral contents of an ore sample using elemental assays as provided by an X-Ray fluorescence (XRF) analyzer. This tool can then be used by the geology department to estimate the mineral contents of ore blocks from the XRF assays of exploration and production of core samples used to characterize the ore blocks of an orebody.

The next step consists of the estimation of the way the minerals are separated by the concentrator. Knowing the mineral recoveries in the concentrator and the mineral composition of the ore, it is fairly straightforward to predict the mill performances associated with the processing of an ore block.

The development and testing of the Mineral Content Estimation (MCE) tool are carried out using data obtained from the concentrator operation. Upon the commissioning of the global geometallurgy tool for the mine, the MCE tool will be applied to the assays of the core samples at the geology level (see Figure 1) to provide the mineral contents of the ore blocks. The estimation of the nominal mineral recoveries is also carried out with daily production data from the concentrator. These mineral recoveries will be used to predict the concentrator performances in terms of metal recovery and concentrate grade as it is the purpose of a geometallurgical predictor.

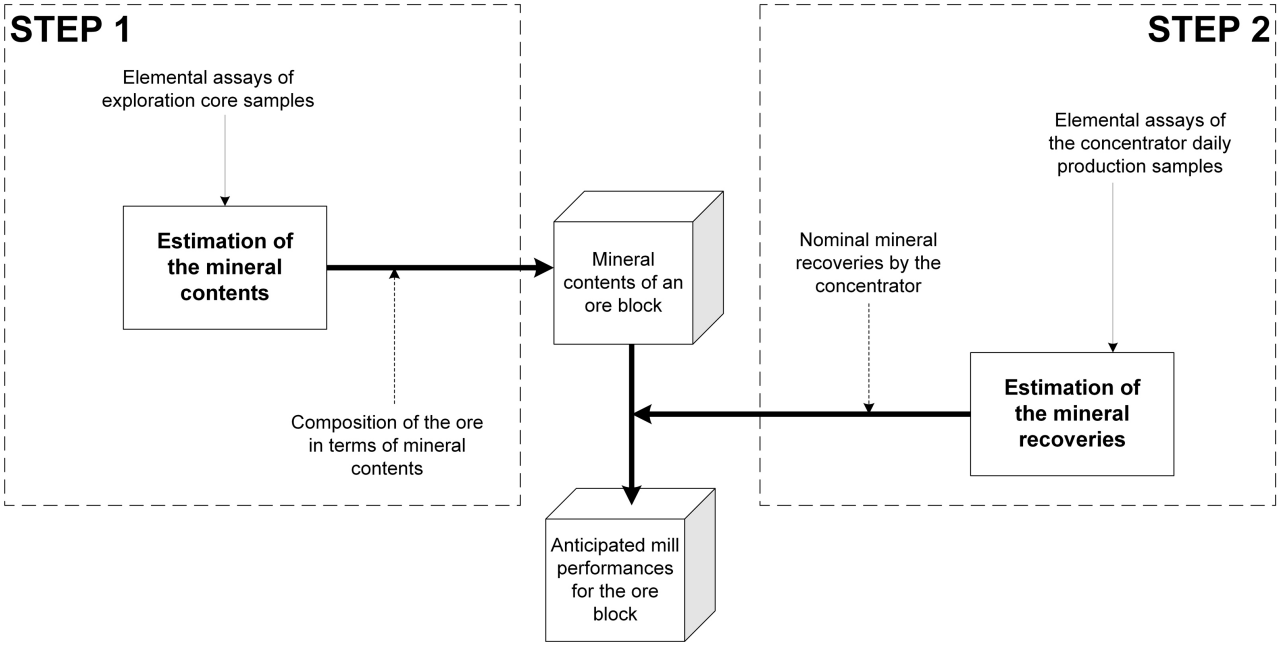

Figure 1. Proposed approach to build a mineral-based ore block model for geometallurgy.

3. Quebec Iron Ore Mine and Concentrators

The Quebec Iron Ore (QIO) mine [4] [5] is located in the Labrador through northern Quebec, Canada (see **Figure 2**). The mine is a subsidiary of the Australian Champion Iron company. The orebody called the Bloom Lake Deposit has been open pit mined by QIO since 2018.

The Bloom Lake Iron Deposit lies within the Fermont Iron Ore District within the geological Greenville Province (see **Figure 2**). The high-grade metamorphism of the Greenville Province is responsible for recrystallisation of both iron oxides and silica in primary iron formation, producing coarse-grained sugary quartz, magnetite, specular hematite schists (meta-taconite), which are characteristics that facilitate the concentration process [4] [6].

The main iron carrier mineral in the ore body is hematite (Fe_2O_3). Magnetite (Fe_3O_4) and the goethite-limonite ($FeO{\cdot}nH_2O$) group are secondary iron minerals with concentrations varying according to the mined location of the orebody. The main gangue mineral is quartz with traces of apatite, carbonates, amphiboles and plagioclases minerals. **Table 1** lists the minerals and their abundance in the ore.

The mined ore is gyratory crushed to −20 cm (−8 inches). The crushed ore is conveyed or trucked to a stockpile from which the ore feeds two parallel lines of autogenous mills in a closed circuit with 5.0 mm and 0.85 mm screens. The material passing the 0.85 mm screen feeds the iron concentration circuit. The concentration circuit is shown in **Figure 3**. The first part of the circuit uses only gravity based equipments, mainly spirals and hydraulic classifiers [6]. The ground ore assaying 30% - 35% Fe, is firstly processed by rougher spirals that yield a concentrate assaying more than 60% Fe, a middling stream (<15% Fe) and a reject

Figure 2. Location of the Bloom Lake deposit (52˚47'00" north, 67˚05'00" west).

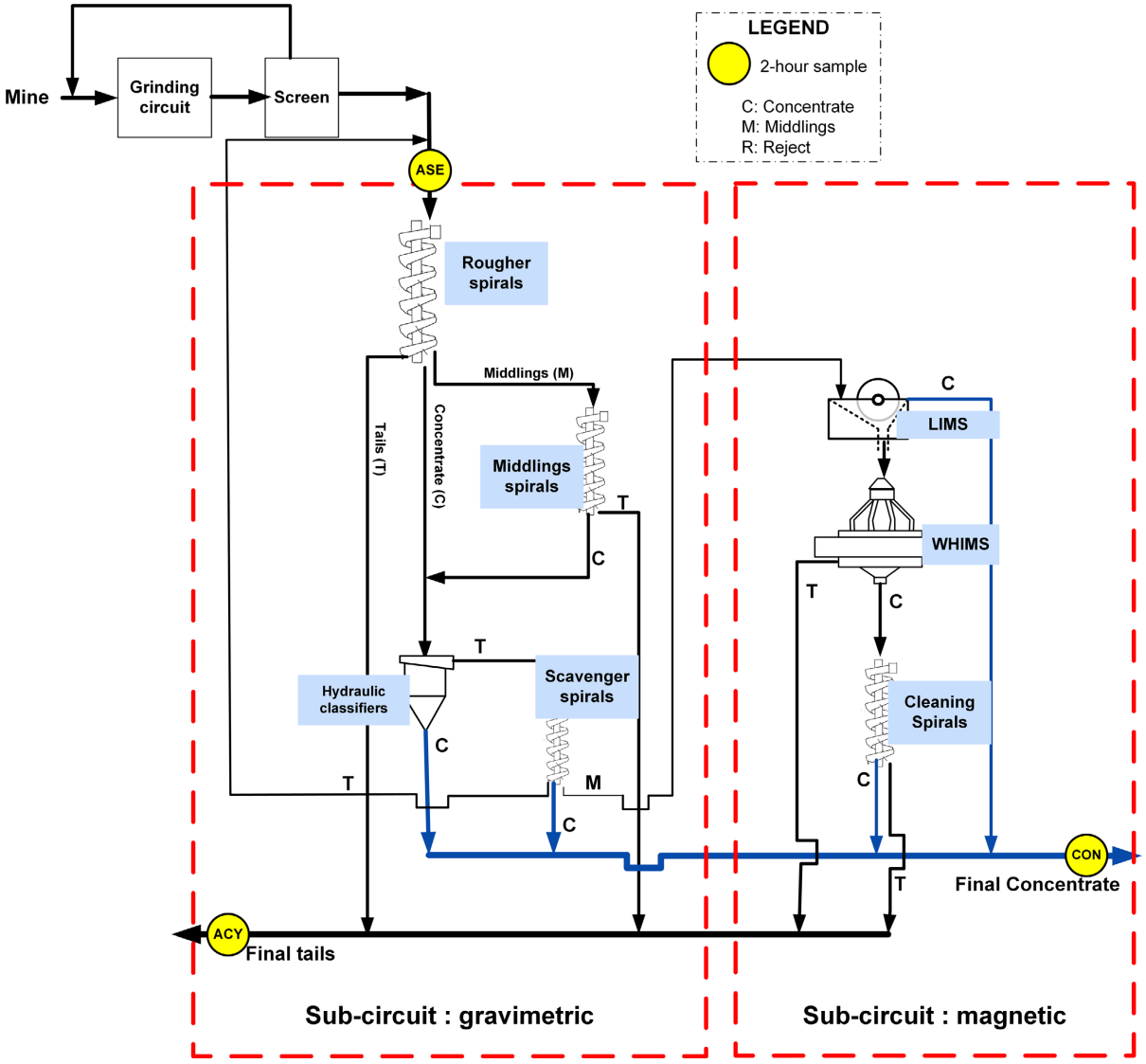

Figure 3. QIO concentration circuit.

Table 1. Identified minerals in the iron ore by QIO [4] [5] [7].

Mineral or group (abbreviation)	Abundance (%)	Formula
Amphiboles (Amp)	0 - 2	
Actinolite		$Ca_2(Mg,Fe)_5Si_8O_{22}(OH)_2$
Cummingtonite		$(Mg,Fe)_7Si_8O_{22}(OH)_2$
Grunerite		$Fe_7Si_8O_{22}(OH)_2$
Hornblende		$(Ca,Na,K)_2(Mg,Fe,Al)_5Si_8O_{22}(OH)_2$
Apatite (Apt)	0 - 2	$Ca_5(PO_4)_3(OH,F)$
Carbonates (Carb)	0 - 2	
Ankerite		$Ca(Fe,Mg,Mn)(CO_3)_2$
Calcite		$CaCO_3$
Dolomite		$CaMg(CO_3)_2$
Hematite (Hem)	30 - 50	Fe_2O_3
Hydrated iron oxides (Goe)	0 - 3	
Goethite		$FeO{\cdot}H_2O$
Limonite		$FeO(OH){\cdot}nH_2O$
Magnetite (Mag)	2 - 8	Fe_3O_4
Mica (Mic)	0 - 2	
Biotite		$K(Mg,Fe,Ti)_3AlSi_3O_{10}(OH,F)_2$
Manganese oxides (MnO_2)	0 - 1	
Pyrolusite		MnO_2
Plagioclases (Plg)	0 - 2	*N/A*
Pyrite (Pyr)	0 - 1	FeS_2
Quartz (Qtz)	40 - 60	SiO_2
Titaniferous minerals (TiMin)	0 - 1	
Ilmenite		$FeO{\cdot}TiO_2$

(<9% Fe) that is directed toward the plant tailings ponds after thickening to recover water that is recirculated back into the grinding circuit. The rougher spiral middling stream feeds a battery of middling spirals that give a concentrate assaying ~59% Fe and a reject (~10% Fe) directed to the tailing's ponds. The rougher spirals concentrate joins the middling spirals concentrate to feed the hydraulic classifiers that produce a concentrate assaying more than 66% Fe (target % Fe > 66%) and a reject stream (~30% Fe) that feeds a battery of scavenging spirals. The scavenging spirals produce: 1) A concentrate (approx 60% Fe) that

joins the hydraulic classifier concentrate into the final concentrate, 2) A middling stream (~10% Fe) consisting of fine hematite, magnetite and quartz that is directed toward the magnetic separation part of the plant (see **Figure 3**) and, 3) A reject stream (<10% Fe and <7% w/w solids) that is reverted to the rougher spirals as a way to recover water.

The middling stream of the scavenging spirals is firstly processed in Low Intensity Magnetic Separators (LIMS) to recover liberated magnetite that would otherwise overload the upstream WHIMS. The LIMS concentrate (~59% Fe) consists mainly of magnetite and is sent to the final iron concentrate. The LIMS reject that is depleted of magnetite feeds Wet High Intensity Magnetic Separators (WHIMS), whose purpose is to recover fine hematite and magnetite lost by the LIMS. The WHIMS reject is sent to the plant tails while the WHIMS concentrate feeds a battery of cleaning spirals whose concentrate is added to the final concentrate whereas the reject is sent to the tailings.

The final concentrate assays more than 66.2% Fe. The iron recovery in the final concentrate is above 80% [5], with more than 77% of the iron minerals recovered in the gravity-based circuit, leaving a 3% to 5% Fe recovery in the magnetic based circuit. The circuit operation is controlled via chemical (elemental) assays of 2-hour samples collected from the rougher spiral feed (ASE), final concentrate stream (CON) and plant reject stream (ACY). These sample locations are shown in **Figure 3**.

4. Advantages of Using a Mineral Composition for a Block Model

Each ore block of the QIO orebody is currently characterized by its Fe and SiO_2 contents as measured by assaying exploration core samples. This section shows that for a complex ore such as the QIO one, in which iron is carried by three minerals that respond differently to the concentration process, the sole knowledge of the iron and silica contents is not sufficient to anticipate the metallurgical performances of the mill for a block of ore.

4.1. Linking the Mill Performance to the Elemental Composition of the Ore

In support of this last proposition, **Figure 4(a)** shows a plot of the iron recovery to the concentrate calculated using the two-products formula [6] [8] applied to the 2-hour assays of the feed, concentrate and reject samples collected on the circuit (See **Figure 3**). The observed iron and silica contents in the mill feed during the same period are also shown in **Figure 4(b)** and **Figure 4(c)**, which consists of more than 8500 observations obtained from January 2019 to February 2021. The period of low iron recovery between observations 3500 and 4000 can hardly be explained by changes in the iron or silica contents of the mill feed.

This hardly observable dependency between recovery and mill feed composition is better shown by the X-Y plots in **Figure 5**. Since the objective of a geometallurgy project is to predict the mill performances using assays of the ore

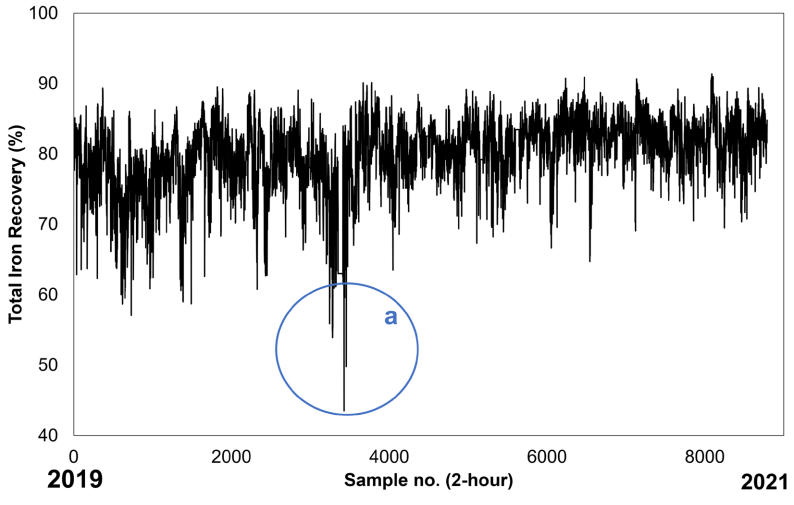

(a)

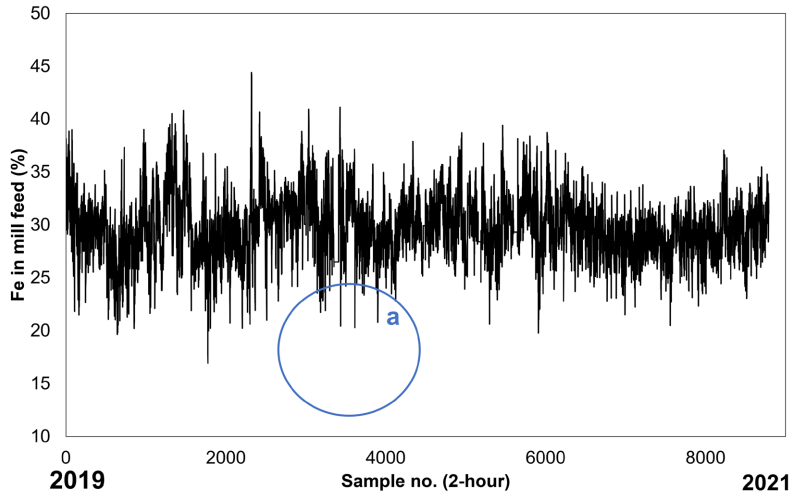

(b)

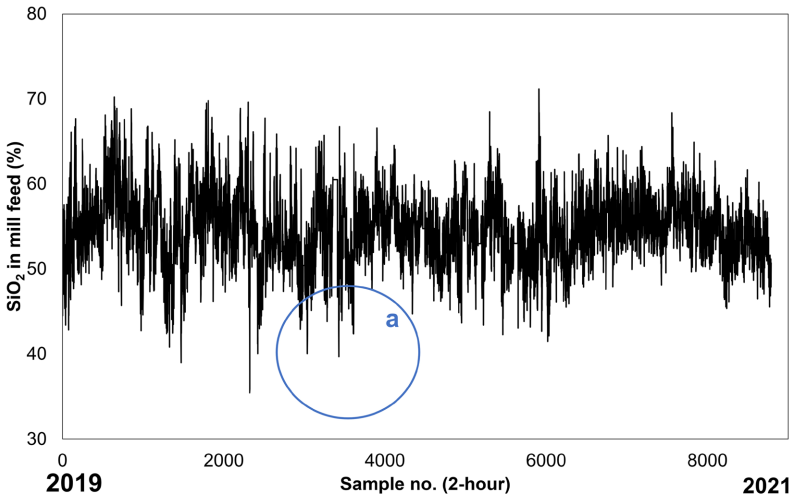

(c)

Figure 4. Trends of iron recovery, iron grade and silica grade in the mill feed from 2019 to 2021. (a) Iron recovery; (b) Iron grade in mill feed; (c) Silica grade in mill feed.

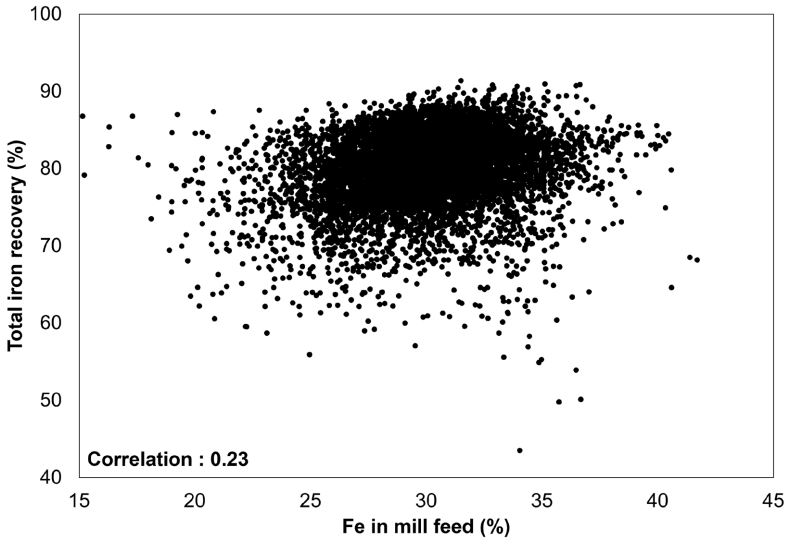

(a)

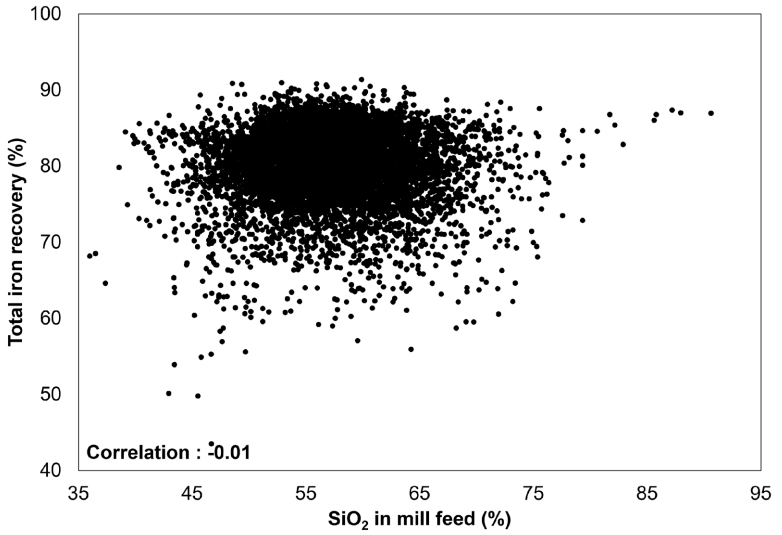

(b)

Figure 5. Absence of visual relationships between the iron recovery and iron/silica grade of the mill feed (8500 observations). (a) Iron grade in mill feed; (b) Silica grade in mill feed.

block model or the mill feed composition, it is obvious that with correlation factors of 0.23 and −0.01 (see **Figure 5**), it will be unlikely possible to achieve the calibration of a robust empirical model to link the iron recovery to the iron and silica contents of an ore block. Indeed, a standard multiple regressions method on the data yielded the empirical model:

$$R_{\mathrm{Fe}} = 1.43 + 0.65x_{\mathrm{Fe},mf} - 0.33x_{\mathrm{SiO_2},mf}, \quad R^2 = 0.18 \tag{1.1}$$

where R_{Fe} is the iron recovery in the final concentrate, $x_{\mathrm{Fe},mf}$ and $x_{\mathrm{SiO_2},mf}$ the iron and silica contents of the mill feed (*mf*). The very low R^2 determination coefficient of 0.18 confirms that the model is not able to adequately predict the iron recovery. The introduction of additional assays (Al_2O_3, K_2O, CaO, MgO, …)

of the mill feed did not improve the capability of the empirical prediction.

The dispersion observed in **Figure 5** found its origin in several sources, namely:

- Unavoidable sampling and assaying errors [8].
- Possible mechanical and operational problems.
- Variations of the iron concentrate grade which is not applicable here as the plant operation is adjusted to maintain a 66.2% Fe content in the final concentrate.
- Ore characteristics that are not accounted for by only the iron and silica contents of the mill feed.

One of the ore disturbing characteristics is the ore texture that can be assessed by a visual examination of the core samples [9]. This texture characteristic can be added as information to the block model, although the challenge remains in the linking of the mill performances to the ore texture [9], a problem that is still awaiting an answer. Another disturbance that is partly accounted for by the elemental assays of an ore block model is the mineral composition of the ore. The usefulness of a mineral characterization of the ore to anticipate the grindability of an ore block is also reported in [2].

4.2. Linking the Mill Performances to the Mineral Composition of the Ore

This last idea applies well to the Quebec Iron Ore mine considered in this paper, in which iron is carried by hematite, magnetite and goethite-limonite whose proportions may vary depending of the location in the orebody. Since these minerals respond differently to the gravity concentration process, the plant iron recovery is intimately linked to the content of these minerals in the mill feed. Indeed, coarse and dense (SG = 5.0) hematite is well recovered in the spirals and hydraulic classifiers, while dense (SG = 5.0) but finer magnetite is less efficiently recovered in these separators. On its side, goethite-limonite tends to be broken into fine particles and the low specific gravity of this mineral (SG = 3.0) negatively hampers its gravity recovery. Using the approach described in the following section with additional measurements to the regularly measured assays it is possible to estimate the concentrations of hematite, magnetite and goethite in the mill feed. The usefulness of this additional information is illustrated with data from a 60-day operation period of the mill.

Figure 6(a) and **Figure 6(b)** show the observed 60-day period trends for the iron and silica contents in the mill feed together with the iron recovery. The iron content of the mill feed shows a typical variation between 34% and 38%, which can hardly be used to explain the Fe recovery excursions away from the average 80% recovery. During the low recovery periods indicated by **a** and **b** in **Figure 6(c)**, the mill operators may spend efforts and time trying to identify the sources of the problem. If the ore block model could provide the basic information on the contents of the critical minerals this information would allow the operators to rapidly make a diagnosis of the problem.

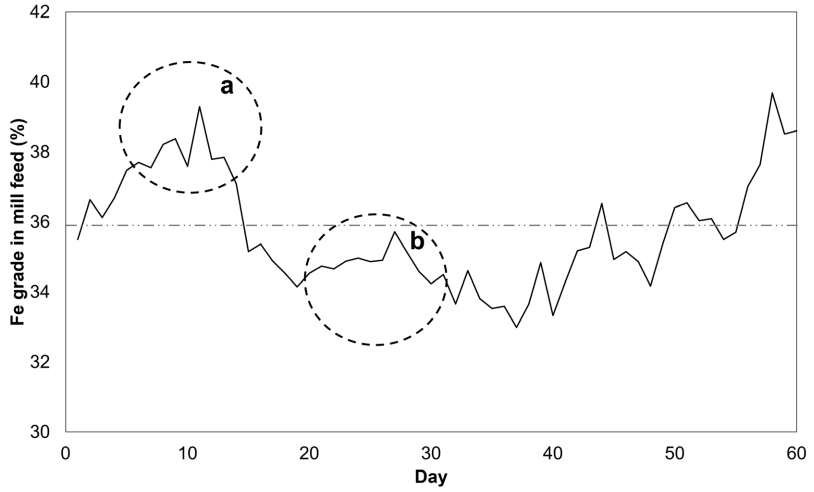

(a)

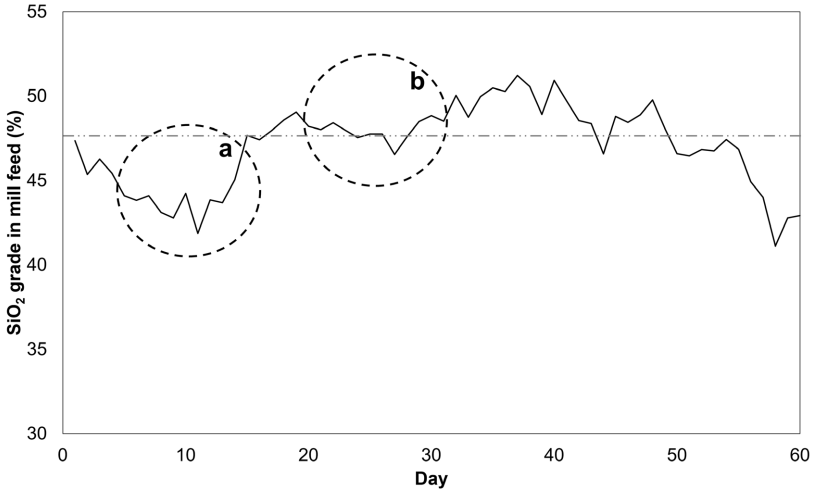

(b)

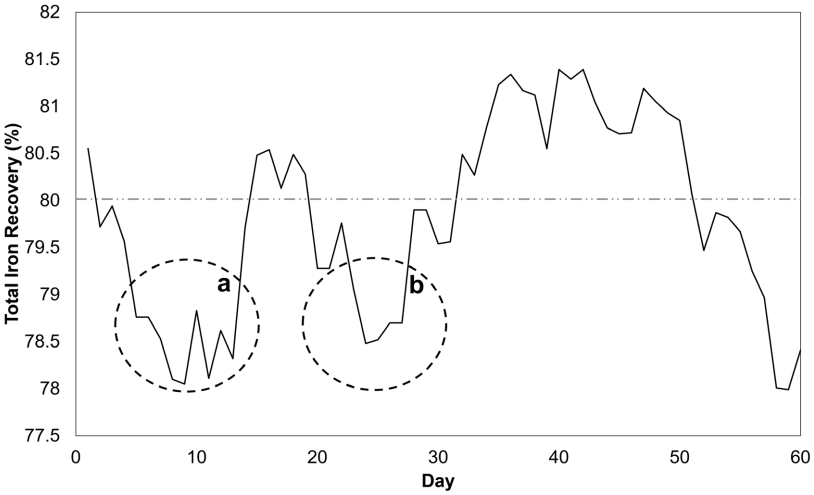

(c)

Figure 6. Explaining periods of low recovery from the iron and silica grades of the mill feed. (a) Iron grade in mill feed; (b) Silica grade in mill feed; (c) Iron recovery to final concentrate.

Indeed, in that particular case, the low recovery situations reproduced in Figure 7(c) overlap with periods of increase in the magnetite and goethite concentrations in the mill feed, as it can be observed in Figure 7(a) and Figure 7(b).

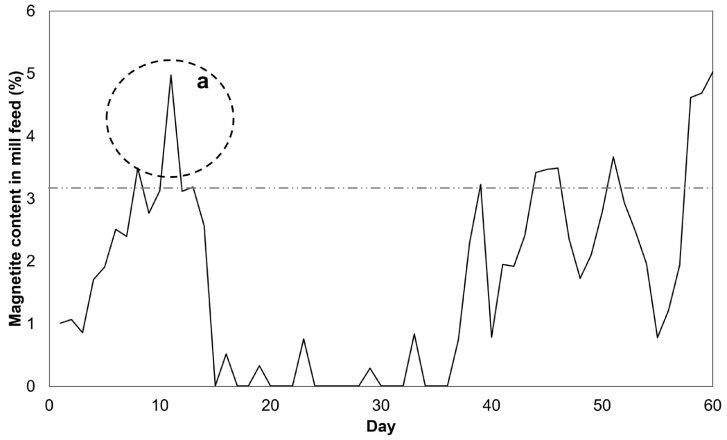

(a)

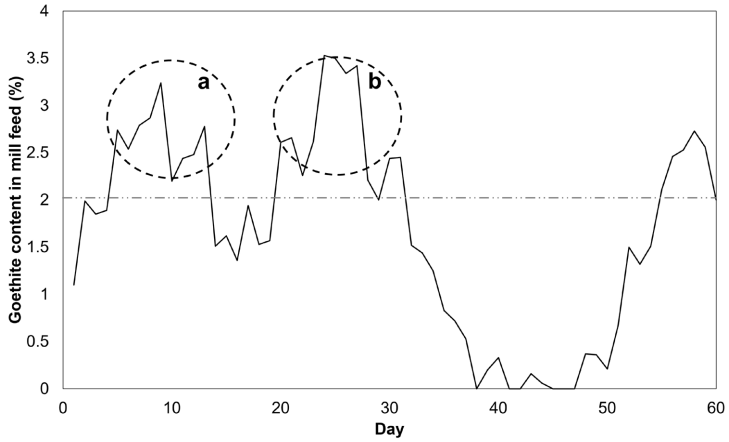

(b)

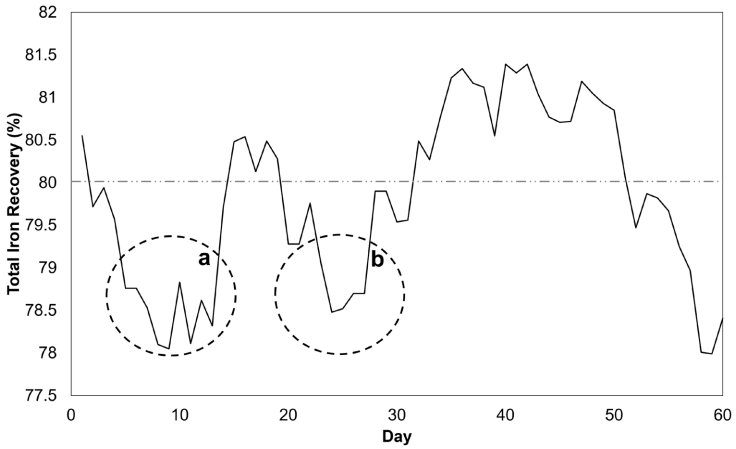

(c)

Figure 7. Explaining periods of low recovery by the poorly gravity recoverable mineral contents of the mill feed. (a) Magnetite content in mill feed; (b) Goethite content in mill feed; (c) Iron recovery to final concentrate.

This example is representative of any ore in which the valuable metal is carried by different minerals behaving differently in the concentration process.

5. Estimation of the Mineral Contents in the Ore

The previous example shows the advantages of describing the ore in terms of mineral contents rather than metal contents. In practice, there are two approaches to estimating the mineral concentrations of a given ore:

- The use of a Mineral Liberation Analyzer (MLA) [7] to obtain a direct measurement of the mineral contents. However, few industrial plants have such equipment and the expertise to use it on the mine site. Also, MLA analysis is time demanding and costly and is not well suited to cope with the large production number of exploration core samples from geology. Other approaches based on image analysis of core samples are currently investigated [9], but the focus of such analysis is more on the identification of the ore texture than on measuring the mineral concentrations.
- The calculation of the mineral contents from elemental assays of the core samples. The geology core samples are usually assayed for building the ore block model; this approach is already more suitable than the MLA one for exploration samples. The key to success lies in the selection of the elements that should be assayed to maximize the data redundancy and the capacity of estimating or "observability" of the concentrations of the strategic minerals.

5.1. Estimation of the Mineral Contents from Elemental Assays of the Ore

The estimation of the mineral contents from elemental assays makes use of the stochiometric or transfer matrix of the ore [7]. The transfer matrix gives the concentration of each assayed element in each mineral or family of minerals (see **Table 1**) considered for the ore. The elements' concentrations are usually measured by XRF. For the QIO ore, the assayed elements are Fe, SiO_2, Al_2O_3, Na_2O, CaO, TiO_2, K_2O, MgO, Mn and P_2O_5. Irregularly Satmagan measurements [10] are also carried out to follow the magnetite content of the samples; the magnetic content for this ore is entirely associated with magnetite (Fe_3O_4). The carbon and sulfur contents are also measured but not on a regular basis. Exceptionally, a Loss on Ignition at 400˚C (LOI400) measurement [11] is carried out. The minerals of the transfer matrix (φ) for the QIO ore are identified in **Table 1**. To maximize the observability [12] of the mineral contents, some minerals are grouped into families. This is the case for the carbonate family that includes calcite, dolomite and ankerite, or for amphiboles (see **Table 1**). The definition of these families implies that only the total carbonate content can be estimated and not the concentrations of the individual carbonate minerals. The transfer matrix used for the QIO ore is given in **Table 2**. The values of the transfer matrix elements are either calculated from the composition of the minerals, when it is known (e.g., Fe in Hematite):

Table 2. Transfer matrix for the QIO ore (see **Table 1** for abbreviations).

Assays[a]	Mag	Goe	Pyr	Carb	Apt	TiMin	Mn Oxide	Mic	Plg	Hem	Amp	Qtz
Fe	0.72	0.51	0.47	0.01	-	0.52	0.24	0.05	-	-	0.07	-
Satmg	1.00	-	-	-	-	-	-	-	-	-	-	-
SiO_2	-	0.02	-	-	-	0.01	-	0.42	0.67	-	0.56	1.00
Al_2O_3	-	0.02	-	-	-	0.002	-	0.17	0.19	-	0.02	-
MgO	-	-	-	0.05	-	-	0.01	0.19	-	-	0.20	-
CaO	-	-	-	0.49	0.55	0.01	-	-	0.09	-	0.11	-
Na_2O	-	-	-	-	-	-	-	-	0.07	-	0.005	-
K_2O	-	-	-	-	-	-	-	0.11	-	-	-	-
TiO_2	-	0.01	-	-	-	0.23	-	-	-	-	0.004	-
Mn	-	0.002	-	-	-	-	0.43	-	-	-	0.002	-
S	-	-	0.54	-	-	-	-	-	-	-	-	-
C	-	-	-	0.12	-	-	-	-	-	-	-	-
P_2O_5	-	-	-	-	0.42	-	-	-	-	-	-	-
LOI400	-	0.90	-	-	-	-	-	-	-	-	-	-

$$\varphi_{\frac{Fe}{Fe_2O_3}} = \frac{2m_{Fe}}{2m_{Fe}+3m_O} = \frac{2\times 55.8}{2\times 55.8+3\times 16} = 0.7 \quad (1.2)$$

where $\varphi_{\frac{Fe}{Fe_2O_3}}$ is the fraction of iron in hematite and m_{Fe} and m_O the atomic mass of iron and oxygen) or measured by microprobe for complex minerals such as amphiboles or plagioclases. The Satmagan is an additional measurement that allows the estimation of the magnetite content, while the LOI400 can be directly linked to the goethite-limonite content as [11]:

$$x_{Goe} = 1.11\times LOI400 \quad (1.3)$$

where x_{Goe} is the concentration of hydrated iron oxides (goethite-limonite) and the LOI400 is expressed in %. The Loss On Ignition at 400˚C (LOI400) is the weight that is lost by the sample when it is heated at 400˚C for 1 hour [13]. For goethite the mass loss is due to dehydration:

$$2FeOOH + heat \rightarrow Fe_2O_3 + H_2O_{(g)} \quad (1.4)$$

The transfer matrix of **Table 2** includes rows to account for carbon and sulfur assays when available. When these assays are not available, the rows are removed from the matrix leading to a reduced observability of pyrite and carbonate contents. Indeed, in the absence of a sulfur assay, the pyrite content estimate is poorly reproducible. The same comment applies to the carbonate content in the absence of a carbon assay.

The problem of the estimation of the mineral contents can thus be stated as:

"*Given a set of elemental assays, Satmagan and LOI400 measurements for an*

ore sample and the transfer matrix, find the corresponding mineral contents of the sample."

Whiten [12] examined various analytical solutions to the problem and applied them to a sulfide ore with a limited number (5) of sulfide minerals of well-known composition and thus for a well-defined transfer matrix. Levesque *et al.* [7] considered different approaches for the case of an iron ore consisting of more than 10 minerals of complex composition and showed that the estimated mineral contents calculated from elemental assays are consistent with MLA measurements. The approach followed here is similar to that of [9] but introduces the idea of weighing the measurements according to their reproducibility and takes advantage of the availability and ease of use of non-linear optimization algorithms such as the Solver macro implemented in Microsoft Excel™.

The estimation of the mineral contents starts with initial guesses for the concentration of $N_m - 1$ minerals. The total number of minerals identified for the ore is noted N_m and the concentration of mineral m is noted y_m. Since the N_m minerals describe the ore in its entirety (or sum up to 100%), the concentration of one mineral can be deduced from the other mineral contents, *i.e.*:

$$\hat{y}_{N_m} = 100 - \sum_{m=1}^{N_m - 1} \hat{y}_m \tag{1.5}$$

where $\hat{y}_m$ stands for the estimated concentration of mineral m in the sample. Estimated elemental assays are readily obtained from the estimated mineral concentrations and the transfer matrix by:

$$\hat{x}_e = \sum_{m=1}^{N_m} \left(\varphi_{e,m} \hat{y}_m \right) \quad \forall e = 1, \cdots, N_e \tag{1.6}$$

where $\hat{x}_e$ is the estimated value for measurement e (% Fe, % SiO_2, …, % Mn, Satmagan, LOI400), N_e is the number of measurements available to estimate the mineral contents and $\varphi_{e,m}$ is the concentration of element e in mineral m or transfer matrix $\{e, m\}$ value. The optimal mineral concentrations should yield estimated elemental assays that are close to the measured values. This proximity is measured by the weighted least squares criterion:

$$\min J\left(\hat{y}_1, \hat{y}_2, \cdots, \hat{y}_{N_m - 1}\right) = \sum_{e}^{N_e} \left(\frac{x_e - \hat{x}_e}{\sigma_{x_e}} \right)^2 \tag{1.7}$$

That should be minimum for the optimal mineral contents $\left(\hat{y}_1, \hat{y}_2, \cdots, \hat{y}_{N_m - 1}\right)$. The variable x_e is the e^{th} measurement and σ_{x_e} is the standard deviation of that measurement. A poorly reproducible measurement is characterized by a large standard deviation and reciprocally, a reproducible measurement receives a small standard deviation. The inverse of the standard deviation in the criterion will thus give more weight to reliable measurements and less to poorly reliable ones.

The estimation of the mineral contents that minimize the criterion of Equation (1.7) is readily carried out using a non-linear optimization algorithm [14] such as the Solver macro implemented in Microsoft Excel™.

5.2. Results of the Application of the Mineral Estimation Method to Mill Feed Assays

The technique is illustrated with data obtained from a sample of the rougher spiral feed stream considered by the mill operators as a good approximation for the fresh mill feed (see Figure 3). For that particular case, Satmagan and LOI400 measurements were obtained in addition to the regular XRF chemical assays. The transfer matrix used is that of Table 2, for which the C and S rows are removed. The available measurements are given in Table 3. A constant 10% relative standard deviation is assumed for all the measurements except those in a low concentration such as Na and P that are likely to be less reliable than the other ones because their concentrations are close to the detection limit of the XRF. Since the focus of the assaying laboratory is put on the assaying of iron and silica, a 1% relative standard deviation is used for these elements. The measurements and the standard deviations are given in Table 3. The estimated mineral contents are given in Table 4, and the estimated values, $\hat{x}_e$, (Equation (1.6)) for the measurements are given in Table 3. Except for alumina (Al_2O_3) and potassium (K_2O) all the estimated values for the measurements are close to the corresponding measurements. If these departures from the measurements were to be systematically observed for Al_2O_3 and K_2O upon repetitive applications of the mineral estimation applied to the QIO ore sample, it could be an indication of a calibration problem of the XRF or that the aluminum and potassium values in the transfer matrix may need an adjustment. This last option is likely as microprobe analyses are often carried out on a limited number of samples and estimated mineral composition may not be representative of the average ore.

Table 5 gives the statistics on the estimated mineral contents for the 8500 samples of the mill feed (see Figure 3) from 2019 to 2021. Since LOI400 measurements

Table 3. Measured and estimated analyses for the rougher spiral feed.

	Measured values (%)	Standard deviation (%)	Estimated values (%)
Fe	30.42	0.304	30.66
Satmg	2.500	0.250	2.496
SiO_2	52.10	0.521	52.59
Al_2O_3	**0.700**	0.120	**0.557**
MgO	0.810	0.131	0.830
CaO	1.010	0.101	1.046
Na_2O	0.009	0.051	0.095
K_2O	**0.100**	0.060	**0.177**
TiO_2	0.112	0.061	0.119
Mn	0.062	0.056	0.071
P_2O_5	0.064	0.056	0.063
LOI400	0.341	0.034	0.342

Table 4. Estimated mineral contents for the rougher spiral feed.

	Mineral content (%)
Mag	2.50
Goe	0.38
Carb	1.19
Apt	0.15
TiMin	0.45
MnO_x	0.15
Mic	1.61
Plg	1.26
Hem	40.2
Amp	2.38
Qtz	49.7

Table 5. Statistics on the estimated mineral contents for 8500 mill feed samples.

Element or mineral[a]	Average	Standard deviation	Minimum	Maximum
FeT	30.0	2.97	12.5	41.7
SiO_2	57.1	5.53	36.0	90.6
Amphiboles	1.908	2.39	0.00	17.6
Apatite	0.12	0.06	0.00	0.61
Carbonates	0.87	1.14	0.00	9.52
Hematite Goethite	39.2	5.24	16.6	63.2
Magnetite	3.34	2.69	0.00	26.7
Mica	0.59	0.72	0.003	16.6
Manganese oxides	0.097	0.078	0.00	1.03
Plagioclases	0.62	0.59	0.001	8.33
Pyrite	0.009	0.024	0.001	0.58
Quartz	53.2	4.33	35.3	71.1
Titaniferous minerals	0.067	0.15	0.00	2.58

[a]Refers to mineral or group of minerals (see Table 1 from regroupees).

are not available for this data, it is not possible to distinguish goethite-limonite group from hematite and these two minerals are lumped into a goethite-limonite-hematite group. The data in Table 5 shows that over the 2-year period, the concentrations of apatite, plagioclase and biotite in the mill feed remain on average below 1%, allowing us to discard the hypothesis that these minerals may be problematic for the operation of the mill. However, the amphibole

content shows a significant variability, a result that supports the intuition of the mill operators that suspect amphiboles to be responsible for periods of difficult operation. The possibility of calculating the ore mineral contents from elemental assays could thus be an asset to ease the diagnosis of operating problems.

Since the mill feed is the mined ore, the same Mineral Content Estimation (MCE) method can be applied to assays of the exploration core samples in order to have a block model consisting of mineral contents rather than elemental assays.

The mineral estimation procedure is also used to estimate the mineral contents in the 8500 samples of the iron concentrate produced from 2019 to 2021. Table 6 gives the statistics on the results. Quartz is the main contaminant of the concentrate followed by carbonates. The other non-Fe minerals do not appear to pose difficulties. This information may help the plant operators to identify which minerals contaminate the concentrate in case of difficulties in maintaining the targeted 66.2% Fe in the concentrate.

6. Prediction of the Mineral Behavior in a Concentration Circuit

Since the goal of geometallurgy is to link the concentrator performances to the ore composition of the ore block, it is then a pre-requisite to have an estimate of the mineral recoveries by the concentrator. The above MCE procedure could be

Table 6. Statistics on the estimated mineral contents for the 8500 concentrate samples collected.

Element or mineral[a]	Average	Standard deviation	Minimum	Maximum
Fe_T	66.5	0.73	58.4	69.0
SiO_2	4.33	0.83	1.47	13.6
Amphiboles	0.11	0.29	0.00	4.56
Apatite	0.054	0.015	0.00	0.14
Carbonates	0.25	0.27	0.00	3.71
Hematite Goethite	86.9	7.15	36.1	98.0
Magnetite	8.14	6.86	0.00	57.14
Mica	0.031	0.034	0.00	0.82
Manganese oxides	0.075	0.070	0.00	1.10
Plagioclases	0.11	0.13	0.00	2.53
Pyrite	0.019	0.054	0.001	1.45
Quartz	4.22	0.86	1.35	13.5
Titaniferous minerals	0.072	0.19	0.00	3.33

[a]Refers to mineral or group of minerals (see Table 1 from regroupees).

combined with a material balance procedure to obtain, in addition to the mineral contents of the feed, reject and concentrate streams, the recoveries of the minerals in the payable product of the plant. This approach takes advantage of the fact that estimated mineral contents in the products of the concentrator should verify the mass conservation. Indeed, the minerals in the mill feed should be conserved in the mill reject and concentrate, *i.e.*:

$$W_{mf}\hat{y}_{m,mf} - W_{rej}\hat{y}_{m,rej} - W_{con}\hat{y}_{con,mf} = 0 \qquad \forall m = 1,\cdots,N_m \tag{1.8}$$

where W stands for a solid flow rate. The subscripts *mf*, *rej* and *con* indicate the mill feed, final reject, and final concentrate. The approach of combining the MCE with a Material Balance (MCE-MB) benefits from the fact that some minerals are selectively separated in the plant. For instance, apatite and biotite that are in low concentrations in the mill feed will exhibit larger concentrations in the mill rejects where they are selectively directed and thus yield larger and possibly more reproducible elemental assays of the gangue elements carried by these minerals than those obtained for the mill feed. This combined mineral content estimation-mass balance, implying that the assays of three samples are linked by a mass conservation constraint, increases the redundancy [15] [16] of the problem compared to the application of MCE to single ore samples. The principle of the MCE-MB is to simultaneously estimate the mineral contents in the mill feed and the proportion ($\hat{P}_m$) of each mineral going to the concentrate or mineral recovery into the concentrate. This data is sufficient for a single node separator as the one shown in **Figure 8** to calculate the mineral contents in the concentrate and reject streams. Indeed, assuming a unitary ore mass feed rate ($W_{mf} = 1.0$) to the circuit, the mass flowrates of the N_m minerals in the concentrate stream are given by:

$$W_{m,con} = W_{mf}\hat{P}_m\hat{y}_{m,mf} = \hat{P}_m\hat{y}_{m,mf} \because W_{mf} = 1.0 \tag{1.9}$$

where $\hat{y}_{m,mf}$ is the concentration of mineral m in the mill feed stream (subscript *mf*). The mass split to the concentrate is:

$$W_{con} = \sum_{m=1}^{N_m} w_{m,con} \tag{1.10}$$

The concentrations of the minerals in the concentrate are readily deduced using:

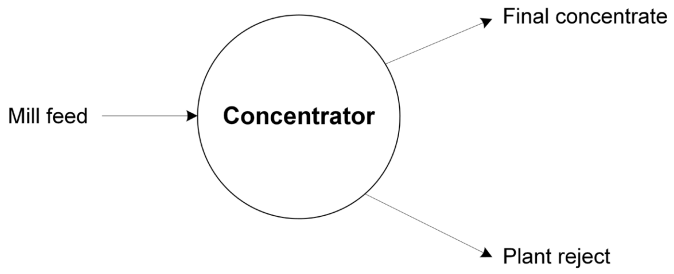

Figure 8. Node separator.

$$\hat{y}_{m,con} = \frac{w_{m,con}}{W_{con}} \qquad \forall m = 1, \cdots, N_m \tag{1.11}$$

The mineral concentrations in the plant reject are obtained from mass balance:

$$\hat{y}_{m,rej} = \frac{\hat{y}_{m,mf} - W_{con}\hat{y}_{m,con}}{1 - W_{con}} \qquad \forall m = 1, \cdots, N_m \tag{1.12}$$

The application of Equation (1.6) to the mineral contents in the reject and concentrate streams gives estimated values for the elemental assays, Satmagan and LOI400 in these streams:

$$\begin{aligned} \hat{x}_{e,mf} &= \sum_{m=1}^{N_m} \varphi_{e,m}\hat{y}_{m,mf} \qquad \forall e = 1, \cdots, N_e \\ \hat{x}_{e,con} &= \sum_{m=1}^{N_m} \varphi_{e,m}\hat{y}_{m,con} \qquad \forall e = 1, \cdots, N_e \\ \hat{x}_{e,rej} &= \sum_{m=1}^{N_m} \varphi_{e,m}\hat{y}_{m,rej} \qquad \forall e = 1, \cdots, N_e \end{aligned} \tag{1.13}$$

The estimated mineral contents in the mill feed ($\hat{y}_{m,mf}$) and the proportions of minerals directed to the concentrate ($\hat{P}_m$) should yield estimates ($\hat{x}_{e,mf}, \hat{x}_{e,con}, \hat{x}_{e,rej}$) that are close to the measurements obtained for the three streams or minimize the weighed least squares criterion:

$$\begin{aligned} &\min J\left(\hat{y}_{1,mf}, \cdots, \hat{y}_{N_m-1,mf}; \hat{P}_1, \cdots, \hat{P}_{N_m}\right) \\ &= \sum_{e=1}^{N_e}\left[\left(\frac{x_{e,mf} - \hat{x}_{e,mf}}{\sigma_{x_{e,mf}}}\right)^2 + \left(\frac{x_{e,con} - \hat{x}_{e,con}}{\sigma_{x_{e,con}}}\right)^2 + \left(\frac{x_{e,rej} - \hat{x}_{e,rej}}{\sigma_{x_{e,rej}}}\right)^2\right] \end{aligned} \tag{1.14}$$

A non-linear optimization algorithm estimates the values of $\hat{y}_{1,mf}, \cdots, \hat{y}_{N_m-1,mf}; \hat{P}_1, \cdots, \hat{P}_{N_m}$ that minimize the criterion of Equation (1.14). The whole procedure can be programmed within one Microsoft Excel™ sheet. In addition to yield estimate of the mineral contents of the mill feed, the MCE-MB gives the recovery of each mineral to the concentrate of the separator, information that can subsequently be used in an ore block model as discussed previously (see **Figure 1**).

The application of the method to the 8500 sets of measurements for the QIO mill feed, concentrate and reject samples yielded the average mineral recoveries given in **Table 7**.

As indicated earlier, in the absence of LOI400 measurements, it is not possible to distinguish hematite from goethite-limonite group, and the estimated recovery for that group is a weighted average of the two mineral recoveries. The 80% recovery for the hematite-goethite group underestimates the hematite recovery that is expected to be efficiently recovered in the process compared to goethite [4]. Magnetite recovery is good at 83.8%, while it was expected that finer magnetite should be less efficiently recovered than hematite in the gravity separation equipments; the better than anticipated magnetite recovery is obviously due to

Table 7. Statistics on the estimated mineral recoveries in the plant concentrate (8500 samples).

Element or mineral[a]	Average	Standard deviation	Minimum	Maximum
Fe_T	80.1	4.89	43.5	91.4
SiO_2	2.87	0.65	0.87	6.74
Amphiboles	11.7	29.4	0.00	65.0
Apatite	23.4	21.4	0.33	89.0
Carbonates	31.5	32.7	0.00	90.0
Hematite Goethite	80.0	4.97	43.1	91.7
Magnetite	83.8	14.7	0.00	93.9
Mica	2.76	6.44	0.00	55.0
Manganese oxides	28.0	11.5	0.00	82.0
Plagioclases	7.31	9.32	0.00	60.0
Pyrite	62.1	15.8	14.2	93.2
Quartz	2.87	0.64	0.86	6.61
Titaniferous minerals	33.1	39.8	0.00	87.0

[a]Refers to mineral or group of minerals (see Table 1 from regroupees).

the LIMS and WHIMS contributions. Low SG minerals such as quartz and biotite are efficiently rejected from the concentrate, while carbonates, apatite and amphiboles may become problematic if their contents in the mill feed increase.

The application of MCE-MB to collected samples of the feed, reject and concentrate streams of each separator (spirals, hydraulic classifiers, LIMS, WHIMS) of the circuit of Figure 3 should yield a better picture of the sources of valuable mineral losses and contamination of the concentrate by gangue minerals.

7. Integration of Mineral Information into an Ore Block Model

The systematic application of the MCE-MB to plant data and MCE to assays of geology samples would allow the generation of the data for an ore block based on ore mineral composition following the approach shown in Figure 9. Additional measurements (e.g., LOI400, C and S assays) may need to be obtained from the regular plant samples to maximize the observability of the concentrations of the strategic minerals. The systematic application of the MCE-MB data processing to the plant sample assays could also allow to fine tune the values of the transfer matrix used by the MCE for the core samples (see Figure 9). MCE-MB typical values for the mineral recoveries will serve to predict the plant performance indices (Fe recovery and concentrate grade) for the ore mineral composition estimated from geology samples (see Figure 9).

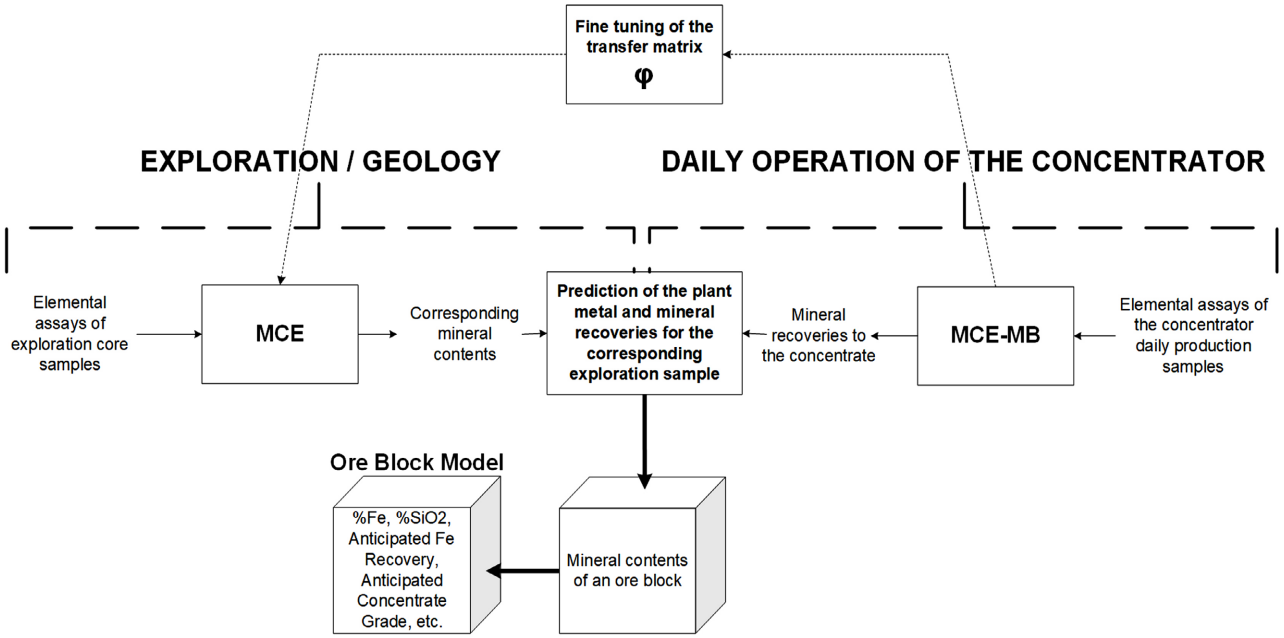

Figure 9. Proposed approach to build a mineral-based ore block model for geometallurgy purposes.

The method is not yet implemented at QIO as detailed sampling [17] [18] shows that the separation of the minerals in the spirals and hydraulic classifiers is not only dependent on the mineral density but also on the mineral particle size. Work is thus on-going to predict the size distribution of the minerals in the ground ore of the concentrator feed. The advantage of introducing particle size into a geometallurgical model is discussed in [3] and [19]. This information will be combined with the gravity separators size-recovery curves [17] [18] to predict the plant operation using a simulator of the whole concentration process.

8. Conclusion

For complex orebodies in which the valuable metal is carried by several minerals that respond differently to the concentration process, an ore block model should not be characterized solely with elemental assays, as this information is not sufficient to anticipate the mill performances while processing the ore block. With a good selection of elemental analyses to be conducted on the production samples, it would not be financially very demanding to add the ore mineral composition into the block model using the mineral content estimation method proposed in the paper. This information could be combined with data on the mineral recoveries observed from daily mill samples used to characterize and control the concentrator operation. A block model providing the mineral composition of the ore, combined with mineral recovery data, could be used to anticipate the mill response to the ore of a block model and facilitate the work of the mill operators, that could then be alerted in advance of periods of difficult ores rather than spending time and energy in trying to identify the causes of poor concentrator performances due to the ore composition.

Acknowledgements

The authors acknowledge QIO for its permission to publish the work. The analytical work by Corem researchers helped in obtaining the transfer matrix for the QIO ore. Finally, the authors are grateful to QIO and the FRQNT for their financial support of the project.

Conflicts of Interest

The authors declare no conflicts of interest regarding the publication of this paper.

References

[1] Lishchuk, V., Koch, P.H., Ghorbani, Y. and Butcher, A.R. (2020) Towards Integrated Geometallurgical Approach: Critical Review of Current Practices and Future Trends. *Minerals Engineering*, **145**, Article ID: 106072. https://doi.org/10.1016/j.mineng.2019.106072

[2] Rincon, J., Gaydardzhiev, S. and Stamenov, L. (2019) Coupling Comminution Indices and Mineralogical Features as an Approach to a Geometallurgical Characterization of a Copper Ore. *Minerals Engineering*, **130**, 57-66. https://doi.org/10.1016/j.mineng.2018.10.007

[3] Suazo, C.J., Kracht, W. and Alruiz, O.M. (2010) Geometallurgical Modelling of the Collahuasi Flotation Circuit. *Minerals Engineering*, **23**, 137-142. https://doi.org/10.1016/j.mineng.2009.11.005

[4] Allaire, A., Leblanc, I., Richard, P.L., Girard, M. and Roberge, P.R. (2019) Bloom Lake Mine Feasibility Study Phase 2. BBA, Montréal.

[5] Lavoie, F. and Verret, F.-O. (2021) Bloom Lake Flowsheet Improvement and Commissioning. *Proceedings of the* 53*rd Annual Canadian Mineral Processors' Conference*, Ottawa, 19-21 January 2021, 102-129.

[6] Wills, B.A. and Napier-Munn, T. (2006) Wills' Mineral Processing Technology: An Introduction to the Practical Aspects of Ore Treatment and Mineral Recovery. 8th Edition, Butterworth-Heinemann, Waltham, 637.

[7] Lévesque, S., Couet, F., Pérez-Barnuevo, L. and Hennessey, C. (2016) Mineralogical Tools for Ore Characterization-Key Data at All Steps of Iron Ore Concentration. *Proceedings of the XXVIII International Mineral Processing Congress* (*IMPC* 2016), Quebec City, 11-15 September 2016, 831-843.

[8] Morrison, R.D. (2008) An Introduction to Metal Balancing and Reconciliation. Julius Kruttschnitt Mineral Research Centre, Indooroopilly.

[9] Pérez-Barnuevo, L., Lévesque, S. and Bazin, C. (2018) Automated Recognition of Drill Core Textures: A Geometallurgical Tool for Mineral Processing Prediction. *Minerals Engineering*, **118**, 87-96. https://doi.org/10.1016/j.mineng.2017.12.015

[10] Rapiscan® Systems (2022) Satmagan 135. https://www.rapiscansystems.com/en/products/satmagan-135

[11] Weissenborn, P.K., Dunn, J.G. and Warren, L.J. (1994) Quantitative Thermogravimetric Analysis of Haematite, Goethite and Kaolinite in Western Australian Iron Ores. *Thermochimica Acta*, **239**, 147-156. https://doi.org/10.1016/0040-6031(94)87063-2

[12] Whiten, B. (2007) Calculation of Mineral Composition from Chemical Assays. *Mineral Processing and Extractive Metallurgy Review*, **29**, 83-97.

https://doi.org/10.1080/08827500701257860

[13] Viczian, I. and Földvári, M. (2011) Handbook of the Thermogravimetric System of Minerals and Its Use in Geological Practice: Occasional Papers of the Geological Institute of Hungary. Geological Institute of Hungary, Budapest.

[14] Press, W.H., Teukolsky, S.A., Vetterling, W.T. and Flannery, B.P. (2007) Numerical recipes: The Art of Scientific Computing. 3rd Edition, Cambridge University Press, Cambridge.

[15] Sadeghi, M., Hodouin, D. and Bazin, C. (2018) Mineral Processing Plant Data Reconciliation Including Mineral Mass Balance Constraints. *Minerals Engineering*, **123**, 117-127. https://doi.org/10.1016/j.mineng.2018.04.023

[16] Bazin, C., Sadeghi, M. and Roy, J. (2016) Tracking Mineral Contents of the Ore from Daily Production Samples. *Proceedings of the* 47*th Canadian Mineral Processors' Annual Conference*, Ottawa, 18-21 January 2016, 32-49.

[17] Sadeghi, M. and Bazin, C. (2020) The Use of Process Analysis and Simulation to Identify Paths to Improve the Operation of an Iron Ore Gravity Concentration Circuit. *Advances in Chemical Engineering and Science*, **10**, 149-170. https://doi.org/10.4236/aces.2020.103011

[18] Bazin, C., Payenzo, G.M., Desnoyers, M., Gosselin, C. and Chevalier, G. (2012) The Use of Simulation for Process Diagnosis: Application to a Gravity Separator. *International Journal of Mineral Processing*, **104**-**105**, 11-16. https://doi.org/10.1016/j.minpro.2011.11.009

[19] Praes, P.E., de Albuquerque, R.O. and Luz, A.F.O. (2013) Recovery of Iron Ore Tailings by Column Flotation. *Journal of Minerals and Materials Characterization and Engineering*, **1**, 212-216. https://doi.org/10.4236/jmmce.2013.15033